THE JOURNAL OF PHYSICAL CHEMISTRY B

Article

pubs.acs.org/JPCB

The Alignment of Barium Ferrite Nanoparticles from Their Suspensions in Electric and Magnetic Fields

Darja Lisjak*[,†] and Simona Ovtar[†,‡]

[†]Department for Materials Synthesis, Jožef Stefan Institute, 1000 Ljubljana, Slovenia

[‡]Jožef Stefan International Postgraduate School, 1000 Ljubljana, Slovenia

Supporting Information

ABSTRACT: The alignment of plate-like barium ferrite nanoparticles, with diameters of 10−350 nm and thicknesses of 3−10 nm, in electric and/or magnetic fields was studied. Stable suspensions were prepared in 1-butanol with dodecylbenzenesulphonic acid as a surfactant. The deposits were produced from the suspensions with classic electrophoretic deposition, electrophoretic deposition in a magnetic field, and with drying in a magnetic field. The experiments, supported by theoretical calculations, show that the alignment of the nanoplates in the deposits was determined by the interplay between the hydrodynamic, electric, and magnetic forces. The preferential alignment of the nanoplates in plane with the substrate coincided with their magnetic orientation, and it increased with the shape anisotropy of the particles. The deposits were sintered at 1150 °C for 5 h to obtain ceramic films, which showed a magnetic orientation up to 90%.

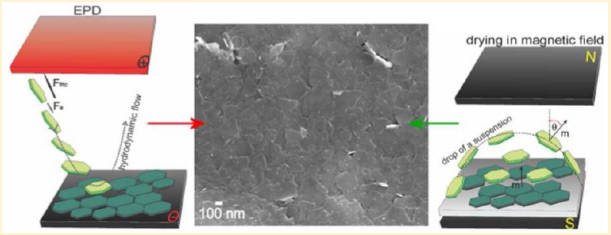

INTRODUCTION

Barium ferrite (BaFe), with the chemical formula $BaFe_{12}O_{19}$, is a ferrimagnetic oxide from the group of hexagonal ferrites or hexaferrites. Its crystalline structure is of magnetoplumbite type and highly anisotropic, with a = 0.589 nm and c = 2.32 nm.[1] As a consequence of this, BaFe crystals grow extensively in the ab-plane, while their growth in the c-direction is limited. Thus, BaFe typically forms thin hexagonal plates. Such a crystal and shape anisotropy inevitably results in anisotropic magnetic behavior, thereby making BaFe suitable for permanent magnets, magnetic recording, self-biased and micro/millimeter-wave applications. However, bulk materials with randomly aligned grains show isotropic magnetic properties. Therefore, the highest magnetic performance can be achieved only in ceramics or films with magnetically aligned grains. Such alignment coincides with the crystallographic orientation, since the magnetic easy axis corresponds to the crystallographic c-axis, which is perpendicular to the plate's plane.

The magnetic alignment of BaFe ceramics is typically achieved by wet pressing while different methods have been studied for the preparation of magnetically oriented films. Pulsed-laser deposition (PLD) and liquid-phase epitaxy (LPE) are both based on the epitaxial growth on a crystallographically matching substrate.[2−5] While only thin films can be obtained with PLD, thicker films can form with the LPE. However, the good magnetic orientation of thicker films was only possible with an additional underlayer, formed by PLD prior to the LPE of BaFe. Screen printing (SP), followed by a low-temperature annealing in a magnetic field, is another method suitable for the preparation of magnetically oriented BaFe thick films.[5,6]

Several studies showed that electrophoretic deposition (EPD) can be applied as an alternative method for the preparation of oriented thick films from anisotropic particles. Crystallographically oriented films were obtained by the alignment of anisotropic TiO_2 particles in an a.c. electric field.[7] Alternatively, diamagnetic TiO_2 and Al_2O_3 particles with anisotropic magnetic susceptibilities can be aligned during the EPD process under a strong magnetic field.[8,9] Constrained sintering accompanied by the anisotropic and abnormal grain growth of the EPD deposits from $BaNd_2Ti_5O_{14}$ rods resulted in oriented sintered films.[10] Recently, it was also shown that the alignment of highly anisotropic plates of $Al(OH)_3$ can be achieved with EPD without using any additional field or thermal treatment.[11] Verde at al., proposed that the hydrodynamic flow during the electrophoresis of thin ZnO plates directed their deposition in the plane with the substrate.[12] The combination of the last three approaches also proved to be efficient in the preparation of magnetically oriented BaFe films.[13]

Since BaFe is a ferrimagnetic material, it seems natural to use a magnetic field for the alignment of the particles. However, the magnetic field also increases the magnetic attraction between the particles and thus enhances the flocculation of particles in a suspension. Therefore, magnetically directed assemblies are typically produced from (super)paramagnetic or even dia-

Special Issue: Electrophoretic Deposition

Received: May 30, 2012
Revised: July 5, 2012
Published: July 26, 2012

   dx.doi.org/10.1021/jp305256t | J. Phys. Chem. B 2013, 117, 1644−1650

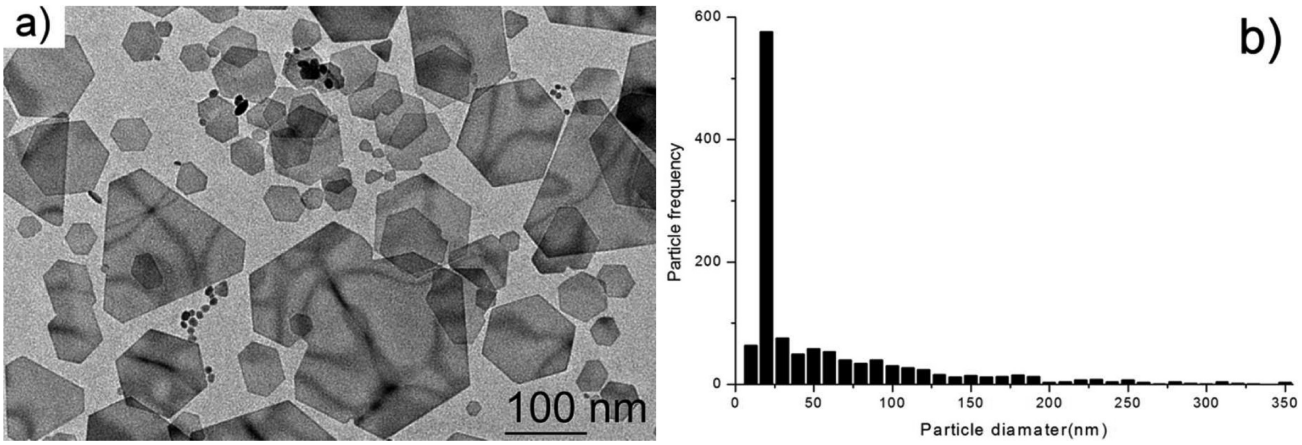

Figure 1. BaFe particles: (a) TEM image and (b) particle-size distribution.

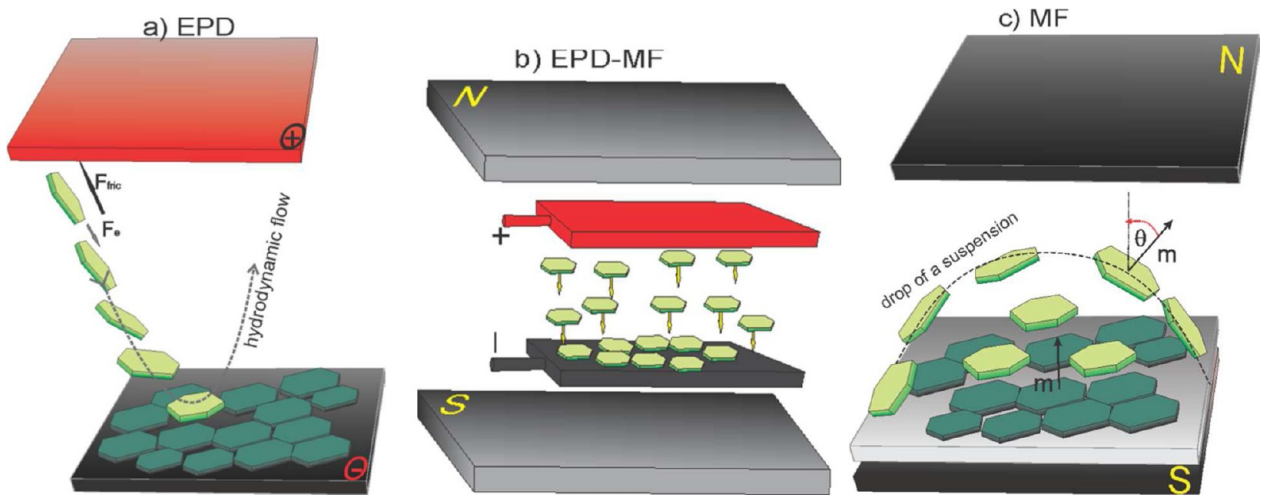

Figure 2. The deposition of BaFe plates from a suspension under different external fields – schematic presentation: (a) electrophoretic deposition (EPD), (b) electrophoretic deposition in a magnetic field (EPD-MF), and (c) drying in a magnetic field (MF).

magnetic particles with weak or no magnetic interparticle interactions.[14,15] It is known that dispersed particles deposit homogeneously on a substrate, while inhomogeneous and porous deposits are obtained from flocculated suspensions. Consequently, a weaker alignment can be expected in the latter case. The purpose of this work was to compare the effect of an electric versus a magnetic field on the alignment of BaFe particles during their deposition. We will show that by tailoring the particles and the suspensions' properties together with the processing parameters, BaFe films with a magnetic orientation of around 90% can be obtained regardless of the type of applied field.

MATERIALS AND METHODS

Particles and Suspensions. Ba ferrite (BaFe) particles were synthesized hydrothermally as described previously.[13] The iron and barium hydroxides with the molar ratio 5:1 were precipitated with sodium hydroxide. The suspension of hydroxides with the addition of dodecylbenzenesulphonic acid (DBSa) was put in an autoclave and heated with a heating rate of 3 °C/h to 240 °C. The autoclave was then naturally cooled to room temperature. The product was washed with water, nitric acid, and acetone. The synthesized powders consisted of thin nanoplates with different diameters and thicknesses (Figure 1).

The morphology of the suspended particles was observed with a transmission electron microscope (TEM, Jeol 2100). For this purpose, a drop of a suspension was dried on a Cu grid. The equivalent diameter of particles was determined from their surfaces with the Gatan Digital Micrograph Software while their thicknesses were directly determined from the TEM images. The measured particles had diameters in the range between 10 and 350 nm. Around 50% particles had diamaters up to 20 nm, and 5% of the particles had diamateres of 200 nm or more (Figure 1). The thickness of the particles ranged between 3 and 10 nm. The magnetic properties of the particles were measured with a vibrating-sample magnetometer (VSM, Lake Shore 7312) up to 1 T. The maximum magnetization, measured at 1 T, was 28 emu/g, and the coercivity was 1620 Oe.

The BaFe particles were stabilized electrosterically with the DBSa in 1-butanol.[16] The ζ-potential of the saturated suspension in 1-butanol were measured with single-point measurements (ZetaProbe Analyzer, North Attleboro and Zeta PALS Zeta Potential Analyzer, Brookhaven Instruments Corporation) taking into account the solvent's dielectric constant (17.84), viscosity (2.99 mPas), and refractive index (1.3993) and was 120 mV. The conductivity (Conductometer Knick–Portamess, cell constant 0.475) of the suspension was 11 μS/cm. The concentration of the suspensions was analyzed after the preparation and after the centrifugation at 5000 rpm

dx.doi.org/10.1021/jp305256t | J. Phys. Chem. B 2013, 117, 1644–1650

by weighing the suspension before and after a heat treatment at 460 °C and was 7 g/L. In this way, the total concentration of the DBSa was also determined, as the DBSa decomposes at 200−460 °C.

Deposits and Films. The deposits were prepared from the stable suspensions with different deposition methods as is schematically presented in Figure 2. The EPD (Figure 2a) was conducted, as previously,[17] in an electrophoretic cell composed of the Al anode and the cathode substrate, which was alumina coated with a 50-nm-thick Pt layer. The deposits were obtained at a constant voltage of 50 V and a separation distance between the electrodes of 7 mm during the deposition time of 15 min. The EPD-MF deposits were obtained when the electrophoretic cell was placed between two permanent magnets (Figure 2b) using the same parameters as above. The magnetic field at the deposition electrode was 0.2 T, and it decreased with the increasing distance from the lower magnet down to a minimum of 0.079 T at a 3-cm separation distance. The deposits were heated to 460 at 0.5 °C/min and annealed at 460 °C for 2 h to remove the organic phase.

In order to elucidate the direct effect of the magnetic field, additional MF deposits were prepared by drying the suspension in a magnetic field of 0.023 T (Figure 2c): 10 drops of a suspension were deposited on a 1 × 1 cm^2 alumina substrate and dried. An additional 10 drops of a suspension were deposited on the dried layer. Such a deposit was then annealed at 460 °C, as described above. The whole process was repeated to obtain a thickness comparable to that of the EPD deposits.

Finally, all the deposits were sintered at 1150 °C for 5 h to obtain ceramic films. In the following, films are named according to the deposition method.

The alignment of the grains in the films was estimated from the magnetic measurements with the VSM, where the magnetic properties were measured out-of-plane (with the magnetic field applied perpendicular to the film plane) and in-plane (with the magnetic field applied parallel to the film plane). The crystallographic orientation of the films was also inspected from the X-ray patterns obtained with an X'Pert PRO diffractometer (PANAnalytical) using CuKα1 radiation. The microstructures of the films were investigated with a scanning electron microscope (SEM, Jeol 7600F).

THEORETICAL BASIS

Let us assume a stable suspension of thin BaFe plates with no interaction between the individual particles, i.e., particles are dispersed in a solvent and not agglomerated. When no external field, electric or magnetic, is applied, the particles move randomly due to the Brownian motion. The gravitational force induces the sedimentation, and the deposition of the sufficiantly large particles on a substrate. A preferential alignment of the plates in the plane with the substrate is expected since such an orientation results in a lower potential energy than for the orientation of plates at any other angle with respect to the substrate. The hydrodynamic force acting on a plate during its motion through a solvent, is related to the hydrodynamic friction, which is assumed to be larger on the plate's basal plane than on its side plane. The hydrodynamic force will cause a hydrodynamic or viscous drag directing a plate in parallel to the hydrodynamic flow.[19] This was studied in more details in refs 20 and 21, and here only an estimation of the hydrodynamic friction effect is considered. The resultant force F (eq 1a), which acts on a particle moving through a solvent with a velocity v, depends on the particle's orientation, which is related to the translational friction coefficient R_{ij} (eqs 1b and 1c).[19] Equations 1b and 1c are valid for the friction coefficients of an oblate spheroid and were used as a good approximation for the friction coefficients on the basal and the side planes, respectively. Here, η is solvent's the viscosity, r is the platelet's diameter, and $h = d/2$ is half of the platelet's thickness d.

$$F = 6\pi\eta R_{ij} v \tag{1a}$$

$$R_{\text{basal}} = \frac{8}{3}\frac{h^2 - r^2}{\frac{2h^2 - r^2}{2\sqrt{r^2 - h^2}}\arctan\left[\frac{\sqrt{r^2 - h^2}}{h}\right] - 2h} \tag{1b}$$

$$R_{\text{side}} = \frac{16}{3}\frac{h^2 - r^2}{\frac{2h^2 - 3r^2}{2\sqrt{r^2 - h^2}}\arctan\left[\frac{\sqrt{r^2 - h^2}}{h}\right] + 2h} \tag{1c}$$

In the steady state, when the hydrodynamic force equals to the gravitational force reduced by the buoyancy, the sedimentation velocity of a plate in two orientations can be calculated as follows:[19]

$$v_{\text{sed}} = \frac{r^2 d(\rho_p - \rho_s)g}{6\eta R_{ij}} \tag{2}$$

Here, $\rho_{p,s}$ denotes the density of a particle and the solvent, respectively, and g denotes the acceleration due to gravity.

The kinetic energy of a particle moving due to Brownian motion is equal to the thermal energy, and the velocity of an oblate spheroid moving randomly due to Brownian motion can be expressed with eq 3.[19,22] Here $k = 1.38 \times 10^{-23}$ J/K is the Boltzmann constant, and T is the absolute temperature. Again we will use the approximation of an oblate spheroid for a plate. By comparing the velocity of a particle due to sedimentation from eq 2 and the Brownian velocity from eq 3, we can estimate the predominant regime of the particle's movement in a suspension in the absence of an applied field. In order to distinguish between the two velocities, we will denote them as v_{sed} and v_{BM}, respectively.

$$v_{\text{BM}} = \sqrt{\frac{2kT}{\pi\eta r}} \tag{3}$$

Additional forces are exerted on a particle when an electric field is applied during the EPD, i.e., the electrophoretic and electro-osmotic forces.[7,12] The electrophoretic force (F_{EP}) originates from an electrostatic attraction between a charged particle and an oppositely charged electrode, i.e., the substrate. The motion of an isolated particle with the surface charge q, the surface charge density σ at the surface area A, and a large Debye length $1/\kappa$ in an unperturbed electric field E can be expressed with eq 4,[18,22] where v_{EPD} denotes the electrophoretic velocity, ζ denotes the ζ-potential, n_∞ is the number density of the dissolved ions, Z is the valency of the ions, and e_0 is the elementary charge.

$$F_{\text{EP}} = qE = \sigma AE = 6\pi\eta R_{ij} v_{\text{EP}}, \quad \text{where}$$
$$\sigma = \frac{4n_\infty Z e_0}{\kappa}\sinh\left(\frac{Ze_0\zeta}{2kT}\right) \tag{4}$$

Equation 4 shows that the electrophoretic force and the velocity of a nonconducting particle does not depend on its size and shape. Therefore the electrophoretic force cannot influence the orientation of the deposited particles. On the contrary,

dx.doi.org/10.1021/jp305256t | J. Phys. Chem. B 2013, 117, 1644−1650

experimental evidence show a direct effect of particle shape on the orientation in a deposit.[7,11,12,23,24] This can only be explained by the effect of the hydrodynamic and electro-osmotic forces (Figure 2a).[7,12,17,24] An anisotropic particle is directed by hydrodynamic forces in such a way that the friction is minimized. Therefore a thin plate is directed in parallel with the flow and in eq 4 $R_{ij} = R_{side}$. However, the direction of the hydrodynamic flow changes in the vicinity of a substrate and redirects the plate in the plane with the substrate (Figure 2a). The electro-osmotic forces originate in the motion of the ions in a double layer. Namely, their net motion is the opposite to that of a particle and creates a local electroosmotic flow of a solvent, which is also opposite to that of a particle. In the vicinity of an electrode a depletion layer forms due to the redox reaction between the ions and the electrode. As a consequence of this, the approaching particles with their double layers are attracted to the electrode and deposit preferentially on empty spaces until they are available.[25] Since plate-like particles of BaFe form columnar agglomerates due to their magnetic attraction in the direction of their easy magnetic axis (i.e., perpendicular to the basal plane), the overall orientation of a deposit is expected to be determined with the orientation of the first deposited layer. In reality, the overall orientation of deposits varies with the thickness (i.e., with the number of deposited layers) because the deposition conditions change for each layer.[24] For example, the deposition rate decreases with the increasing thickness of a deposit due to an increasing resistivity, and particles have more time to adopt the energetically most favorable orientation (i.e., in plane with the substrate). Consequently, the newly deposited layers show higher orientation degree than the former ones. The situation may be reversed at high voltages when particles do not have enough time to align in the plane with a substrate due to the fast deposition rate. In such a case, the large fraction of the misaligned particles from the first layer induces an even stronger misalignment of the subsequent layers.

When the suspension is dried in a magnetic field, the hydrodynamic flow can be neglected, but the plates align in the plane with the substrate due to the magnetostatic force (Figure 2c). As mentioned before, the magnetic easy axis of the BaFe coincides with its crystallographic *c*-axis, which is perpendicular to the plate's basal plane. The particles align with their easy axes parallel to the applied magnetic field. If θ is the angle between the particle's magnetic moment (m) and the applied magnetic field (H), the magnetostatic interaction can be expressed with eq 5.[26] Here M_s is the saturation magnetization, ρ_p is the particle's density, and $\mu_0 = 4\pi \times 10^{-7}$ J/A^2 m is the permeability of free space. Due to the very large magnetocrystalline anisotropy, the demagnetizing field in the case of the BaFe platelets can be neglected.[26]

$$E_m^H = -\mu_0 mH \cos\theta, \quad \text{where} \quad m = M_s \rho_p \pi r^2 d \tag{5}$$

The influence of the magnetic field on a particle can be evaluated by a comparison with the thermal energy and is given by eq 6.[27] A particle is magnetically oriented at a high enough product of mH when $\xi_M > 1$. This means that a lower magnetic field is required to orient larger particles with large magnetic moments than for the smaller or even superparamagnetic particles with small magnetic moments.

$$\xi_M = \frac{\mu_0 mH}{kT} \tag{6}$$

When a high enough magnetic field is applied during the EPD, with the orientation shown in Figure 2b, the magneto-static interaction prevails over the hydrodynamic effect, and the BaFe plates align in the plane with the substrate (i.e., perpendicular to the hydrodynamic flow). Consequently, their velocity, $v_{EP\text{-}MF}$ (eq 7), is reduced in comparison to the v_{EP}, and a greater degree of alignment for the deposited particles is expected, when compared to classic EPD. Since the difference between the hydrodynamic friction on the basal and the side planes increases with the increasing shape anisotropy, i.e., with the increasing diameter-to-thickness ratio, we predict that the magnetic field will affect more significantly the alignment of the larger plates than the smaller ones.

$$F_{EP} + F_M = \sigma AE + \mu_0 mH/L = 6\pi\eta R_{basal} v_{EP\text{-}MF} \tag{7}$$

Here, L denotes the distance between a magnetic pole and a particle. The strongest magnetic force acts on the BaFe plate, which is aligned perpendicular to the magnetic field direction, when the magnetic easy axis or the magnetic moments are aligned in parallel with the magnetic field, $\theta = 0°$ (also see eq 5).

RESULTS

The degree of alignment of the films was evaluated from the anisotropy in their magnetic behavior. Table 1 lists the relevant magnetic properties of the studied films. A significant difference between the magnetic properties measured in the two different perpendicular directions and the high out-of-plane remanent-to-saturation magnetization (OUT Mr/Ms) both suggest a high degree of magnetic orientation of the films. As an example, we also show the magnetic hysteresis loops of the B-MF films (Figure 3a). The OUT loop shows the magnetic saturation (Ms) and the larger remanent magnetization (Mr, i.e., the remaining magnetization at zero magnetic field) as well as the larger coercivity (Hc, i.e., the field required to reverse the magnetization), while the film was not magnetically saturated and showed smaller Mr and Hc values, when measured in plane (IN). Such anisotropic behavior suggests the preferential alignment of the plates in plane with the substrate. The larger the fraction of aligned plates, the higher the OUT Mr/Ms ratios and the Hc values, while, at the same time, both IN properties are low. Therefore, similar preferential alignment of the BaFe plates in plane can be suggested for all the films. The Ms values of the films (34 emu/g) are larger than that of the as-synthesized powder (28 emu/g). This could be expected since the crystallinity, and consequently magnetic properties, of magnetic materials usually improve with the additional thermal treatment (in our case 460 and 1150 °C). In contrast to this, the B-MF film showed lower Ms (18 emu/g) than the as-

Table 1. Magnetic Properties of Films, Sintered at 1150 °C for 5 h, Measured with the Magnetic Field Applied Out-of-Plane (OUT) and In Plane (IN) with the Film

		OUT		IN	
film	Ms (emu/g)	Mr/Ms	Hc (Oe)	Mr/Ms	Hc (Oe)
EPD[17]	34	0.83	3274	0.29[a]	2544
EPD-MF	34	0.84	2579	0.27[a]	2155
MF	18	0.85	3577	0.43[a]	3494

[a]Instead of the Ms, the magnetization measured at 10 kOe was considered when the films did not saturate up to the maximum applied field.

dx.doi.org/10.1021/jp305256t | J. Phys. Chem. B 2013, 117, 1644−1650

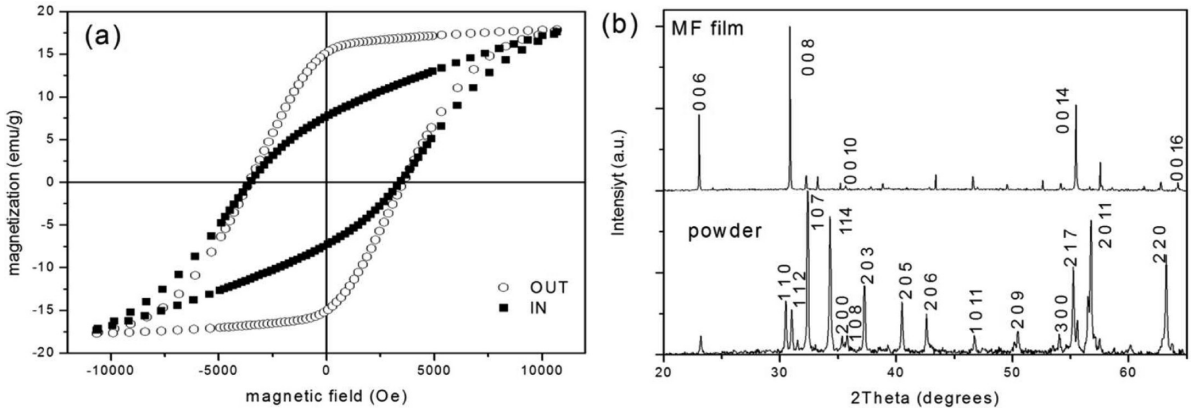

Figure 3. Magnetic hysteresis loops (a) of the MF film sintered at 1150 °C for 5 h with corresponding XRD pattern (b). As a comparison, the XRD pattern of the BaFe sintered powder is also shown. Indices correspond to the BaFe structure, space group $P6_3/mmc$ (194).

synthesized powder. Here, the particles were deposited directly on the alumina substrate (with no Pt layer as in the case of the EPD and EPD-MH films), which can react with the BaFe above 1100 °C. As a consequence of this reaction, Fe^{3+} in the $BaFe_{12}O_{19}$ is partly substituted by Al^{3+}, which decreases the Ms.[28]

As described in the Introduction, the magnetic anisotropy of BaFe is a consequence of its crystalline anisotropy. This is demonstrated in the corresponding X-ray (XRD) diffractogram (Figure 3b). The preferential orientation of the crystallites is indicated by the very high relative intensities of the *00 l* peaks. Their relative intensities are significantly higher than those from a randomly oriented powder and confirm the alignment of crystallites in plane with the substrate.

The preferential alignment of the BaFe plates in the plane was also confirmed with the SEM observations. As an example, we show the surface of the MF film (Figure 4) with the majority of grains aligned in a plane. We can see that sintered film is composed of submicrometer and micrometer-sized grains. This means that during the sintering, most of the grains grew by approximately 1 order of magnitude (see also Figure 4c for comparison). Only a few misaligned grains can be seen on the surface of the MF film, and the image in Figure 4a was selected specifically to show those grains. This is in agreement with the highly anisotropic magnetic behavior of the MF film (Table 1). Some of the grains retain their plate-like shape, as can be seen from the misaligned grain in the center of Figure 4a, while some of the grains appear less anisotropic. These "round" grains are in fact sintered columnar agglomerates (see the magnified image Figure 4b) and are formed from particles shown in Figure 4c. The later image shows more clearly the high degree of the preferential alignment of the individual BaFe particles in the MF film prefired at 460 °C. This temperature was too low for the sintering and high enough for the degradation of the DBSa and therefore enabled us to observe individual particles. Similar morphologies were also observed for the other films.

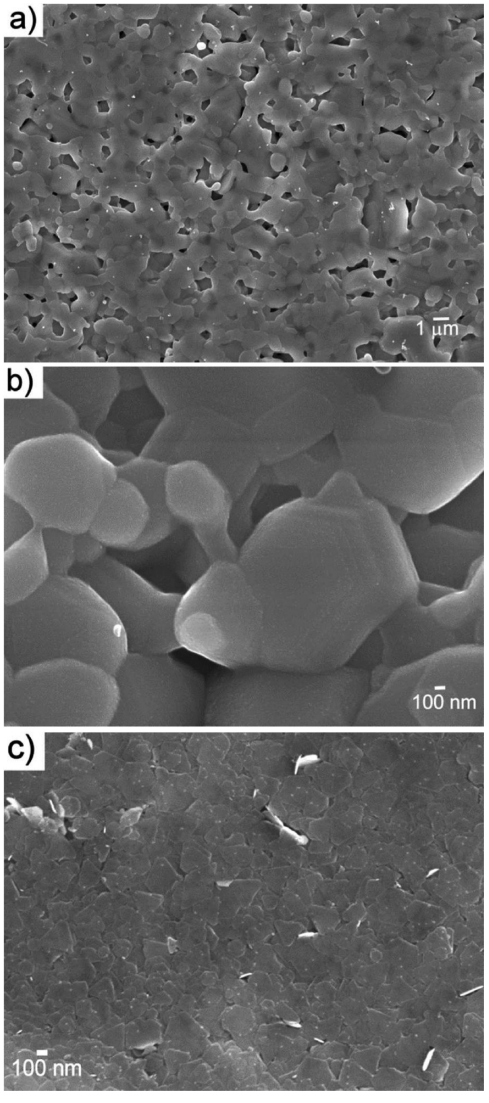

Figure 4. Secondary electron image of the surface of the MF film: (a) sintered at 1150 °C with a magnified view (b), and (c) prefired at 460 °C.

DISCUSSION

Let us now inspect the different parameters that influenced the alignment of the BaFe nanoplates. The minimum and maximum particle sizes, together with the most frequent particle size (Figure 1), were considered in the calculations. Since the Brownian and electrophoretic velocities both exceed the sedimentation velocity by several orders of magnitude (Table 2), the effect of gravity can be neglected. It should be noted that an average sedimentation velocity for the two friction coefficients (R_{basal} and R_{side}) was considered (eq 2).

dx.doi.org/10.1021/jp305256t | J. Phys. Chem. B 2013, 117, 1644−1650

Table 2. The Calculated Parameters That Affect the Motion and the Direction of the Alignment of the BaFe Plates with Different Sizes

$2r/d$	10/3	20/3	50/6	100/6	350/10
R_{basal}/R_{side}	1.03	1.24	1.29	1.40	1.45
v_{BM}/v_{sed}	1.9×10^6	7.7×10^5	9.9×10^4	3.7×10^4	3.4×10^4
v_{EP}/v_{BM}	1.31	2.85	10.6	27.0	167
$v_{EP\text{-}MF}/v_{BM}$	1.27	2.28	8.25	19.4	115
F_E/F_M	1.9×10^6	4.9×10^5	1.6×10^5	1.1×10^5	4.8×10^4
$\xi_{M\text{-}MF}$	3.62	45.3	847	4.5×10^3	1.2×10^5
$\xi_{M\text{-}EPD\text{-}MF}$	12.4	155	2.9×10^3	1.6×10^4	4.0×10^5

As expected for a thin plate, the friction coefficient (Table 2) on its basal plane is larger than the friction coefficient (eq 1b) on its side plane (eq 1c). The ratio between the former and the latter (R_{basal}/R_{side}) increases with the increasing shape anisotropy, i.e., with the increasing diameter-to-thickness ($2r/d$) ratio. Therefore, it can be expected that during the electrophoresis the plates align preferentially in the direction of the hydrodynamic flow (Figure 1a), as has already been suggested in refs 12 and 24. Consequently, R_{side} was included in eq 4 for the calculation of the electrophoretic velocity. We can see in Table 2 that the electrophoretic velocities for the BaFe nanoplates are larger than the corresponding Brownian velocities ($v_{EP}/v_{BM} > 1$). Therefore, all the BaFe plates are affected by the electric field. The plates move toward the oppositely charged substrate where they preferentially deposit in the plane of the substrate as a consequence of the hydrodynamic and electroosmotic forces (as explained in theory and calculations). This explains the high magnetic anisotropy of the EPD film (Table 1).

When the EPD was performed in the magnetic field (Figure 2b), the plates preferentially aligned in parallel with the substrate already during the electrophoresis and, as such, they were also deposited on the substrate. Namely, the magnetic easy axis, which is perpendicular to the plate's basal plane, tends to align in the direction of the applied magnetic field. This means that the BaFe plates were exposed to a larger hydrodynamic friction (R_{basal}) than in the case of classic EPD (R_{side}) and, therefore, they moved more slowly toward the substrate than in the case of classic EPD (Table 2: $v_{EP} > v_{EP\text{-}MF}$). Consequently, the EPD-MF film produced under the same conditions as the EPD films was thinner than the latter, around 8 and 17 μm, respectively. For all the plates, even for the smallest ones, the parameter $\xi_{M\text{-}EPD\text{-}MF} \gg 1$ (Table 2), which suggests that the magnetostatic energy is significant in comparison to the thermal energy. Consequently, the magnetic orientation of the EPD-MH films should be higher than that of the EPD films. In contrast to expectations, a similar magnetic orientation was measured for the EPD and EPD-MF films (Table 1). This suggests that the applied magnetic field does not affect only the individual particle, but also the interparticle interaction. The external magnetic field increases the magnetic dipole−dipole interaction potential between the particles, which can lead to the (partial) agglomeration of the particles. The largest magnetic dipole−dipole attraction between the BaFe plates is exerted between their basal planes (with the antiparallel alignment of their magnetic moments) and columnar agglomerates can be formed (Figure 4b). The larger the particles, the larger the magnetic attraction between them, and the formation of agglomerates in the magnetic field is more probable. Therefore, the effect of the magnetostatic force on a single particle was reduced by its effect on the magnetic dipole−dipole interaction.

Table 2 shows that the magnetic force (F_M) on a particle is negligible in comparison to the electric force (F_E). This was the reason that in the case of the EPD-MF process the velocity of the plate was calculated as the electrophoretic velocity with the friction coefficient on the basal plane (see eqs 4 and 7). At the same time, the low magnitude of the magnetic force suggests that the deposition of the studied BaFe plates would be much slower in the absence of an electric field. This was confirmed with an experiment, similar to the one shown in Figure 2b, although in this case no electric field was applied. Only a very thin deposit, which did not cover the substrate completely, was obtained after 24 h. Therefore, further tests on the effect of the magnetic field on the alignment of BaFe plates were conducted, as shown in Figure 2c.

Similar to the EPD-MF samples, in the MF samples, the BaFe plates also align preferentially in parallel with the substrate. However, in the latter case, the main driving force for their alignment is the magnetostatic force. It is clear from eq 5 that the magnetostatic energy is directly related to the magnetic moment of a particle and the strength of the applied magnetic field. The latter was the same for all the samples, while the former increases with the volume of a particle. As mentioned before, the demagnetizing fields due to the shape anisotropy can be neglected for the BaFe plates. Consequently, the effect of the magnetostatic energy increases with the increasing particle size as is observed with the increasing $\xi_{M\text{-}MF}$ value (Table 2). This suggests that the overall alignment of the BaFe plates is governed by the large particles and was confirmed with a parallel experiment, where only small particles (with average size 12 ± 4 nm and M_{1T} of 1.0 emu/g) were deposited and dried in magnetic field (see Supporting Information for details on the preparation and properties − Tables S1 and S2). The MF film from such small particles showed similar magnetic properties in both measured directions (Table S3 in Supporting Information), which suggest on poor preferential alignment of the small particles. However, the larger particles in the original suspension can be destabilized in a magnetic field, as discussed above. Since the applied magnetic field (0.023 T) was lower than that for the EPD-MF process (0.079−0.2 T), the agglomeration degree must have been smaller. The partial agglomeration of the deposited BaFe plates and consequently their misalignment in the MF film (Figure 4b) can explain why their magnetic orientation is only comparable, and not superior, to the EPD film.

Therefore we can conclude that the magnetically oriented BaFe films can be produced with EPD or by drying in the magnetic field, while the application of a magnetic field during the EPD has no advantage in comparison to the classic EPD.

dx.doi.org/10.1021/jp305256t | J. Phys. Chem. B 2013, 117, 1644−1650

CONCLUSIONS

The effect of electric and magnetic fields on the alignment of thin ferrimagnetic barium ferrite nanoplates was studied. The shape anisotropy of the plates resulted in anisotropic hydrodynamic friction coefficients, due to which the plates aligned parallel to the hydrodynamic flow during the electrophoresis, and they deposited in plane with the substrate. This induced anisotropy in the magnetic properties of the films. The application of a magnetic field during the electrophoresis reoriented the plates perpendicular to the hydrodynamic flow and decreased the deposition rate while at the same time it increased the agglomeration of the plates, which diminished the expected preferential alignment of the plates. Otherwise, the magnetic field had no direct effect on the deposition rate since the induced magnetic force was significantly smaller than the electric force. The magnetic field alone induced the preferential alignment of barium ferrite plates during the drying of the suspensions in the magnetic field. The alignment effect increased with the size of the plates, but at the same time it was decreased due to the increasing agglomeration. The later was successfully limited by the combination of high-quality suspensions and weak magnetic field. We can conclude that the alignment of the barium ferrite plates is determined by the interplay of the external and interparticle forces.

Regardless of the deposition method, the films with a magnetic orientation of around 90% can be prepared, and as such they are suitable for self-biased applications. The EDP of barium ferrite nanoplates is proposed for the preparation of thick films where a conductive substrate is required, while the drying in a magnetic field is suitable for applications based on nonconductive substrates.

ASSOCIATED CONTENT

Supporting Information

Preparation procedure of the MF films from small particles, properties of the small particles (Table S1), their suspensions (Table S2), and films (Table S3). This material is available free of charge via the Internet at http://pubs.acs.org.

AUTHOR INFORMATION

Corresponding Author

*Address: Jožef Stefan Institute, Department for Materials Synthesis, Jamova 39, 1000 Ljubljana, Slovenia. E-mail: darja.lisjak@ijs.si.

Notes

The authors declare no competing financial interest.

ACKNOWLEDGMENTS

This work was financially supported in part by the Ministry for Higher Education, Science and Technology of the Republic of Slovenia through the FERFIT project MNT-ERA.Net, 3211-10-000028, and in part by the Slovenian Research Agency. We acknowledge the CENN Nanocenter for the use of the TEM.

REFERENCES

(1) Braun, P. B. *Philips Res. Rep.* **1957**, *12*, 491−548.
(2) Lu, Y. F.; Song, W. D. *Appl. Phys. Lett.* **2000**, *76*, 490−492.
(3) Yoon, S. D.; Vittoria, C. *J. Appl. Phys.* **2003**, *93*, 8597−8599.
(4) Kranov, Y. A.; Abuzir, A.; Prakash, T.; McIlroy, D. N.; Yeh, W. J. *IEEE Trans. Magn.* **2006**, *42*, 3338−3340.
(5) Harris, V. G.; Chen, Z.; Chen, Y.; Yoon, S.; Sakai, T.; Gieler, A.; Yang, A.; He, Y.; Ziemer, K. S.; Sun, N. X.; Vittoria, C. *J. Appl. Phys.* **2006**, *99*, 08M911 (5 pp.).
(6) Chen, Y.; Sakai, T.; Chen, T.; Yoon, S. D.; Geiler, A. L.; Vittoria, C.; Harris, V. G. *Appl. Phys. Lett.* **2006**, *88*, 062516 (3 pp.).
(7) Mittal, M.; Furst, E. M. *Adv. Funct. Mater.* **2009**, *19*, 3271−3278.
(8) Uchikoshi, T.; Suzuki, T. S.; Iimura, S.; Tang, F.; Sakka, Y. *J. Eur. Ceram. Soc.* **2006**, *26*, 559−563.
(9) Suzuki, T. S.; Uchikoshi, T.; Okuyama, H.; Sakkam, Y.; Hiraga, K. *J. Eur. Ceram. Soc.* **2006**, *26*, 661−665.
(10) Fu, Z.; Vilarinho, P. M.; Wu, A.; Kongon, A. I. *Adv. Funct. Mater.* **2009**, *19*, 1071−1081.
(11) Lin, T. H.; Huang, W.; Jun, I. K.; Jiang, P. *Chem. Mater.* **2009**, *21*, 2039−2044.
(12) Verde, M.; Caballero, A. C.; Iglesias, Y.; Villegas, M.; Ferrari, B. *J. Electrochem. Soc.* **2010**, *157*, H55−H59.
(13) Ovtar, S.; Lisjak, D.; Drofenik, M. *J. Am. Ceram. Soc.* **2011**, *94*, 3373−3379.
(14) Grzelczak, M.; Vermant, J.; Furst, E. M.; Liz-Marzan, L. M. *ACSNano* **2010**, *4*, 3591−3605.
(15) Lisiecki, I.; Pileni, M. P. *J. Phys. Chem. C* **2012**, *116*, 3−14.
(16) Ovtar, S.; Lisjak, D.; Drofenik, M. *J. Colloid Interface Sci.* **2009**, *337*, 456−463.
(17) Lisjak, D.; Ovtar, S. *Langmuir* **2011**, *27*, 14014−14024.
(18) Pugh, R.; Bergstom, L. *Surface and Colloid Chemistry in Advanced Ceramics Processing*; Marcel Dekker, Inc.: New York, 1994.
(19) Probstein, R. F. *Physicochemical Hydrodynamics*, 2nd ed.; John Wiley & Sons, Inc.: Hoboken, NJ, 2003.
(20) Hubbard, J. B.; Douglas, J. F. *Phys. Rev. E* **1993**, *47*, R2983−R2986.
(21) Ortega, A.; Garcia de la Torre, J. *J. Chem. Phys.* **2003**, *119*, 9914−9919.
(22) Li, D.; Daghighi, Y. *J. Colloid Interface Sci.* **2010**, *342*, 638−642.
(23) Ohshima, H. *J. Colloid Interface Sci.* **1997**, *185*, 131−139.
(24) Ovtar, S.; Lisjak, D.; Drofenik, M. *Colloids Surf., A* **2012**, *403*, 139−147.
(25) Solomentsev, Y.; Boemer, M.; Anderson, J. L. *Langmuir* **1997**, *13*, 6058−6068.
(26) Stoner, E. C.; Wohlfarth, F. R. S.; Wohlfarth, E. P. *Phil. Trans. R. Soc. London, Ser. A 826* **1948**, *240*, 599−642.
(27) Satoh, A.; Sakuda, Y. *Mol. Phys.* **2009**, *107*, 1621−1627.
(28) Mishra, D.; Anand, S.; Panda, R. K.; Das, R. P. *Mater. Lett.* **2004**, *58*, 1147−1153.